

Computational Analysis for Investigating the Effects of Circular Cavity in a Supersonic Combustor

Ajay Sampath H A¹, Dr. N Chikkanna²

PG Student, Department of Aerospace Propulsion Technology, VTU, CPGS, VIAT, Muddenahalli,
Chikkaballapura, India¹

Professor, Department of Aerospace Propulsion Technology, VTU, CPGS, VIAT, Muddenahalli,
Chikkaballapura, India²

ABSTRACT: The computation aims at studying the effects of circular cavity in its different flow regimes i.e. open, closed and transitional flows depending on the L/D of the cavity and compared with its computed rectangular cavity counter parts. Since there has not been many research in circular cavity, the closely related cavity i.e. rectangular cavity is used for comparison. The flow has been computed for an inlet Mach number of 3 and a stagnation pressure of 6.9bar, the L/D ratios used are 5.5 open flow, 10 transitional flow and 13 closed flow. This study also includes a computation on fuel injection at a distance of 8 mm from cavity, the fuel is injected from an injecting surface of 1mm with a total pressure of 14bar. This further aids in understanding the fuel mixing for all variant of cavities. An attempt is made to provide some guidelines for the future research of circular cavity flame holders.

The study concludes that as we increase the L/D ratio, the cavity effect diminishes in closed and transitional flows for circular cavity and in closed flow for rectangular cavity. The flow requirement such as not having the generation of series of compression waves in the higher L/D and detachment of compression waves at the aft wall is seen in the circular cavity. The fuel distribution is promising in open flow for circular cavity, the fuel distribution in rectangular cavity is promising in open and transitional flows

KEYWORDS: Supersonic combustion, Cavity, L/D ratio, Mach, Combustor, Pressure gradient

I. INTRODUCTION

In the current scenario we have high expectation in the field of aerospace engineering for the applications of high speed aircraft. To meet this requirement we have come up with various technological advancements in jet engines, rocket engines and hybrid engines etc. Pertaining to jet engines the supersonic jet engines are ram jet and scram jet engines, these engines enable us to reach greater speed; sometimes even up to Mach 6 which is about 7000km/hr.

Ram/Scram jet engines greatly differ from the traditional jet engines, they do not have any movable parts like turbine and compressor. Since they travel at high speeds the major concern is the drag loads that affects them. Therefore a mechanical structure in the inlet or in diffuser is only placed to reduce the velocity and increase the pressure of the air entering the combustion chamber. This has to be done because the residence time for the fuel in the combustion chamber is in the order of milli-seconds, therefore it is important for the velocity of the air to be reduced at this stage to prevent the fuel particle from going out of the combustor even before it is combusted.

The usage of mechanical structure is limited based on the Mach number and it cannot be used at higher Mach numbers since it will also induce heavy drag and eventually cause melt down. To overcome this problem we need to use an aerodynamic design within the combustor to decelerate the air entering the combustion chamber. The major type of design that is under study and used is the cavity based combustor. These cavities disturb the flow regime and induce

International Journal of Innovative Research in Science, Engineering and Technology

(A High Impact Factor, Monthly, Peer Reviewed Journal)

Visit: www.ijirset.com

Vol. 7, Issue 8, August 2018

turbulence, circulations and shocks within the combustor which in turn influence in decelerating the air in the combustor. The drag produced by cavity is very less compared to the mechanical structure, hence it favours the requirement at higher speed.

The air-inlet for a scramjet engine has a free stream Mach number of about 6-7 which has to be decelerated to a Mach number of about 2 at entry to the combustor. The main challenges in a scramjet are listed below

- Shorter Fuel residence time because of the high flow velocity
- Mixing of fuel and air at molecular level
- Time required for the chemical reaction to occur
- Evaporation time in case of liquid fuels
- Time of heat release to produce thrust

II. LITERATURE REVIEW

Cavity induces a recirculation zone in supersonic combustor. When fuel is injected at a distance in front of the cavity, cavity provides a pressure drop which facilitates constant ignition or what we call as the flame holding action. The basic idea behind a cavity is; when decelerating inlet air, the usage of a physical body leads to huge drag, which can be avoided by using cavity. While it has that major advantage it also has a drawback which reduces the total temperature and stagnation pressure. Since we will opt for wall injection in many of the cavity based injection system the penetration of fuel into air is also restricted. However, it has to be noted that the mixing efficiency and combustion is significantly enhanced because of the upsurge in heat and mass movement inside the cavity along the shear layer.

Cavity flow regimes

Maureen B. Tracy et al ^[8] have clearly explained the various cavity flows and their behaviour for different L/D ratios.

1. Open Cavity: The cavity in this regime has good depth and hence it is termed open cavity, the flow field in supersonic speeds and the shear layer formed is generally above the cavity. This sort of flow occurs in a flow where the $L/D < 10$, the flow nearly extends above the cavity creating an almost even pressure distribution inside the cavity.
2. Closed cavity: This flow occurs in cavity whose $L/D > 13$, it is termed closed cavity because of its lean depth. This allows more products to enter into the cavity, the flow in the upstream attaches to the cavity floor at some point near it, and then further downstream it gets detached and flows away from the cavity floor. There is low pressure in upstream of the cavity wall because of the flow vicinity and the cavity maintains an average static pressure distribution, while there is high pressure in the downstream wall because of the shear layer impingement. Because of this radical change in pressures up wall and down wall of the cavity there is a huge drag loss.
3. Transitional Cavity: This cavity lies in between an open cavity and closed cavity, it is named transitional cavity since it is the transitional phase between open to a closed cavity. This flow occurs in cavity whose $L/D \sim (11-13)$, the flow field is broken down by the impingement and the downstream shock wave into a distinct sole shock and the reduction in the average pressure distribution. The shock can be seen not attached to the cavity floor, while having the flow impinged on the cavity bottom wall. The pressure gradient in this cavity vary adversely, from a very small change in value of L/D to closed cavity ratio a series of compression waves are produced.

International Journal of Innovative Research in Science, Engineering and Technology

(A High Impact Factor, Monthly, Peer Reviewed Journal)

Visit: www.ijirset.com

Vol. 7, Issue 8, August 2018

III. MODEL

Physical Model

The geometric information of the physical model that has been designed in designer module of workbench is discussed here, a typical 2D supersonic combustor is used as the physical model. The combustor dimensions used are listed in table 1 and a sample combustor design for L/D 5.5 is shown in the figure-1.

Table 1 Combustor dimensions

Inlet height	32mm
Distance from inlet to cavity	220mm
Depth of cavity	8mm (fixed)
Length of cavity	44mm, 80mm, 104mm (variable)
Step height	0.2mm
Outlet	62mm
Distance from cavity to outlet	450mm



Figure-1 Physical model of rectangular and circular cavity combustor (L/D 5.5)

The computation is carried out for three different cases by varying the L/D parameter. The L/D parameter is based on the cavity flow regimes which are open, transitional and closed cavity flows. The depth of the cavity is fixed at 8 mm and the length of the cavity is varied to obtain different flow regimes. The varying lengths used are 44 mm, 80 mm and 104 mm. The L/D ratios hence obtained are 5.5, 10 and 13 respectively. Further the computation is extended with fuel injection from an injecting surface of 1 mm at a distance of 8 mm in front of the cavity. This gives us an insight on how the fuel distribution occurs in all of these cases.

Meshed model

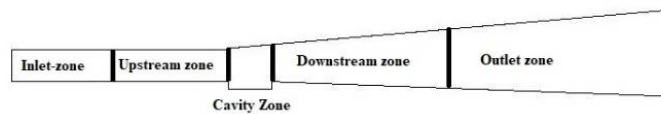


Figure-2 Zone divisions

The physical model has been divided into 5 different zones to maintain a quality mesh and the time of computation. Therefore, the inner most zone; the cavity zone has the least count for mesh sizing and the outer most zone; the inlet-outlet zone has maximum sizing.

Table 2 Mesh Functions

Size function	Proximity – Curvature
Smoothing	High
Span angle centre	Fine
Proximity Size function	Face and edges
Mesh method	Quad dominant
Mesh type	Surface mesh

International Journal of Innovative Research in Science, Engineering and Technology

(A High Impact Factor, Monthly, Peer Reviewed Journal)

Visit: www.ijirset.com

Vol. 7, Issue 8, August 2018

The above listed functions are used to define the meshing, and the same has been incorporated for all other cases. A mesh sample is shown in the figure-3 for both rectangular and circular cavity combustor for L/D ratio of 5.5



Figure-3 Meshed models of rectangular and circular cavity combustor

Mesh statistics: Since there is variation in L/D, the number of nodes and elements are varied. The table 3 has information on various mesh nodes and elements for different cases

Table 3 Mesh Statistics

	L/D	Nodes	Elements
Rectangular cavity	5.5	85829	84764
	10	102922	101791
	13	109245	108090
Circular Cavity	5.5	84984	83949
	10	97490	96406
	13	104853	103742

IV. SETUP

Boundary conditions

The inlet boundary conditions are based on various studies, in particular with experiments and numerical studies conducted by Gruber et al^[1] for supersonic flows. The inlet boundary conditions used are as shown in the table. The operating pressure is set at 18,784 pa which is obtained from inlet to exit pressure ratio following an adiabatic process using the compressible flow equation (1) P_0/P and Stagnation Pressure is at 6.9 bar. The inlet conditions and fuel inlet conditions are listed in table 4 and 5 respectively.

$$P_0/P = [1 + (\gamma - 1) M^2 / 2]^{(\gamma - 1) / \gamma} \dots \dots \dots (1)$$

Table 4 Inlet Conditions

Gauge static pressure	6,71,216 pa
Mach number	3
Temperature	300k
Turbulent kinetic energy	1 m ² /s ²
Specific dissipation rate	1 1/s

Table 5 Fuel Inlet Conditions

Total pressure	14 bar
Temperature	300k
Turbulent kinetic energy	1 m ² /s ²
Specific dissipation rate	1 1/s

Computational Setup

It is vital to have an accurate computational setup since the solution obtained is mainly dependent on the mesh quality, boundary conditions and also the method of solving within the computational software. In this study the computational software used is FLUENT module of ANSYS 17.0 which utilizes Reynolds-averaged Navier–Stokes equations to solve the given problem. The air inlet here is Mach 3, therefore it is vital to choose a proper solver setting to compute the turbulence, compressed flow and shocks.

International Journal of Innovative Research in Science, Engineering and Technology

(A High Impact Factor, Monthly, Peer Reviewed Journal)

Visit: www.ijirset.com

Vol. 7, Issue 8, August 2018

The present computation uses a density based solver, the turbulence model most suited for modelling such high velocity flows is $k-\omega$ SST turbulence model and the same has been employed. (SST) Shear Stress model $k-\omega$ has a combination function to gradually convert from standard $k-\omega$ model near the wall to a great Reynolds number of $k-\epsilon$ model in the outward section of boundary layer. It contains a unique devising for viscosity which interprets the transport effects for the primary turbulent shear stress. This model precisely predicts the zones of separation for intense pressure gradient.

V. RESULTS

In this section, we look at different results obtained after computation of the supersonic combustor in rectangular cavity and circular cavity with 3 variations in L/D of 5.5, 10 and 13. The L/D ratio of 5.5 signifies open cavity flow, 10 transitional cavity flow and 13 closed cavity flow. The contours give us an idea to predict the flow in all three variations for both the cavity cases. The contours plotted below are pressure, velocity, and kerosene species.

Pressure variation

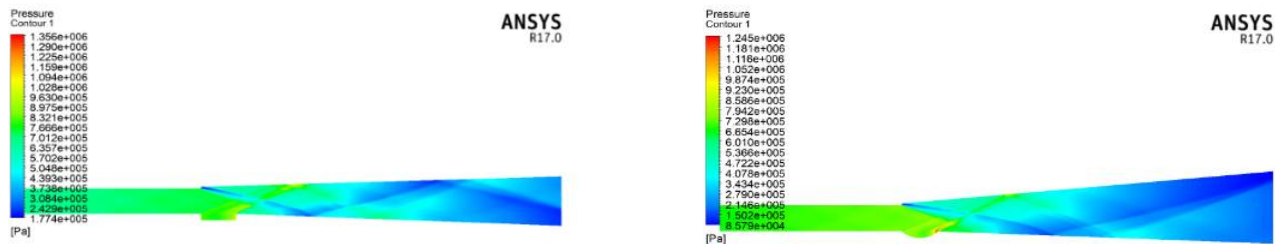


Fig 5.1a Pressure contours Rectangular-CircularCavity L/D 5.5

The above contours shows us the pressure variation across rectangular and circular cavity whose L/D ratio is 5.5 therefore giving us the open cavity flow regime.

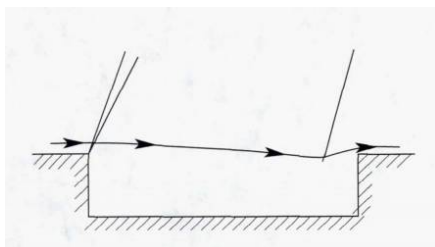


Fig 5.1b Open cavity flow source Maureen B. Tracy et al^[8]

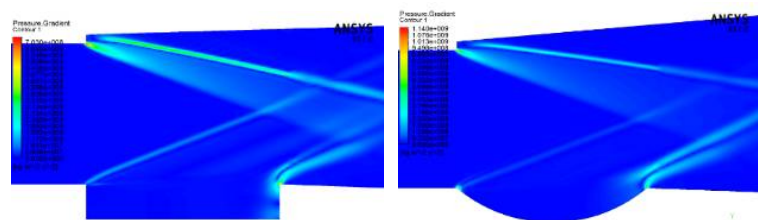


Fig 5.1c Computed Pressure Gradient Rectangular-CircularCavity L/D 5.5

The expected cavity flow and shock formation for open cavity is shown in the fig 5.1b obtained from studies conducted by Maureen B. Tracy et al^[8]. Comparing it with our computed results shown in the fig 5.1c, we can observe the shock formation on both the end walls of the cavity. The shear layer has just span over the cavity as it is expected in both the cases of rectangular and circular cavities.

International Journal of Innovative Research in Science, Engineering and Technology

(A High Impact Factor, Monthly, Peer Reviewed Journal)

Visit: www.ijirset.com

Vol. 7, Issue 8, August 2018

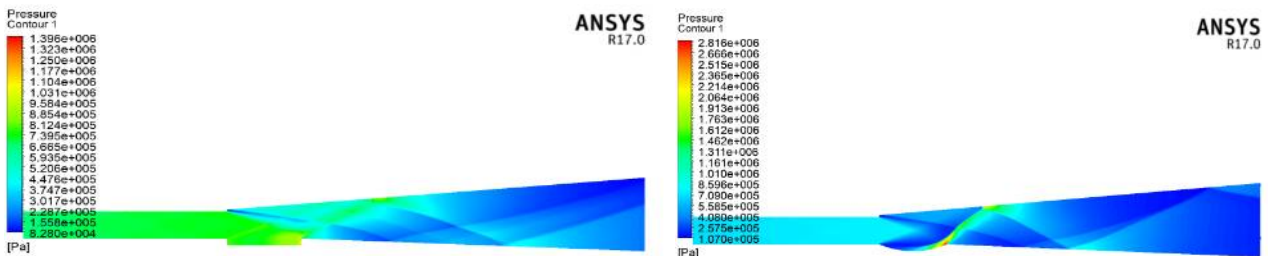


Fig 5.2a Pressure contours Rectangular-Circular Cavity L/D 10

The above contours shows us the pressure variation across rectangular and circular cavity whose L/D ratio is 10 therefore giving us the transitional cavity flow regime.

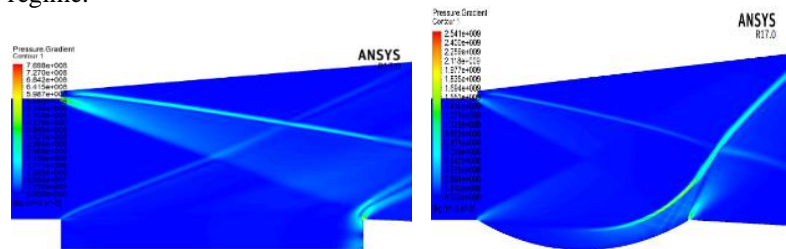
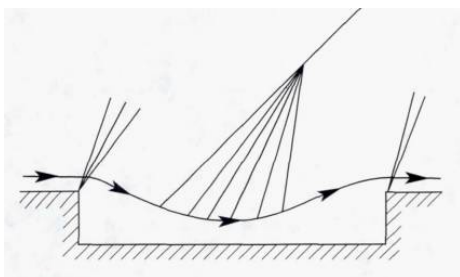


Fig 5.2b Transitional cavity flow source Maureen B. Tracy et al^[8] Fig 5.2c Computed Pressure Gradient Rectangular-Circular Cavity L/D 10

The computed rectangular transitional cavity flow shown in fig 5.2cc agrees with the expected transitional cavity flow shown in the fig 5.2b, while the circular transitional cavity flow has given a different result. I.e. in the circular cavity we can observe that the shock near the aft wall of the cavity has detached and is stronger, this could be because of the geometric shape of the circular cavity. The shear layer is not attached to the cavity floor in both the cases.

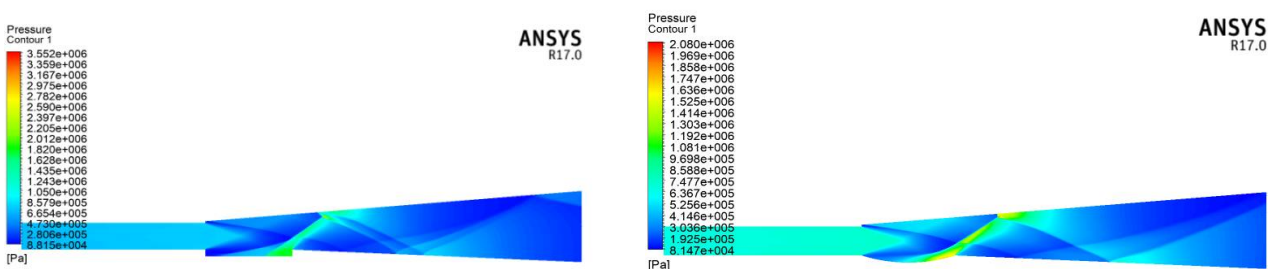


Fig 5.3a Pressure contours Rectangular-Circular Cavity L/D 13

The above contours shows us the pressure variation across rectangular and circular cavity whose L/D ratio is 13 therefore giving us the closed cavity flow regime

International Journal of Innovative Research in Science, Engineering and Technology

(A High Impact Factor, Monthly, Peer Reviewed Journal)

Visit: www.ijirset.com

Vol. 7, Issue 8, August 2018

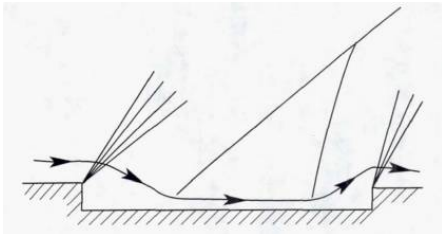


Fig 5.3b Closed cavity flow source Maureen B. Tracy et al [8]

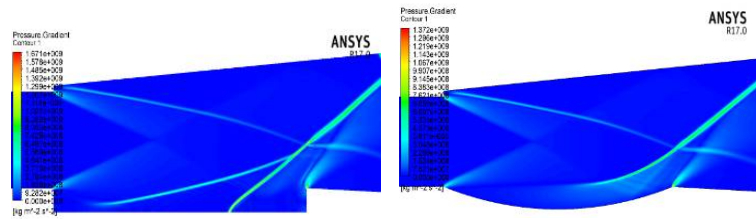


Fig 5.3c Computed Pressure Gradient Rectangular-Circular Cavity L/D 13

The computed results for rectangular closed cavity flow shown in fig 5.3c has shock entering in to the cavity, which is expected as seen in fig 5.3b. Whereas the circular cavity still has a detached shock at the cavity aft wall and is still not attached to the cavity floor. Thus concludes because of the geometric design of the circular cavity, the compression shocks formed in the downstream do not attach to the cavity floor. This signifies the importance of angled aft wall that is used in rectangular cavities to prevent the shear layer from attaching to the cavity floor.

Velocity variation

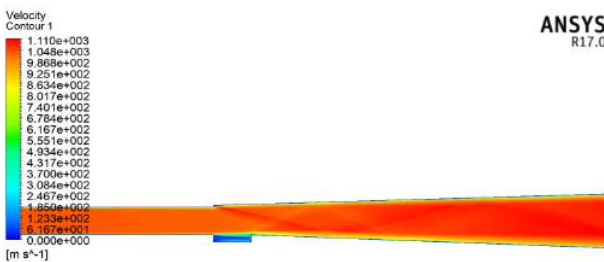


Fig 5.4a Velocity contours RectangularCavities of L/D 5.5

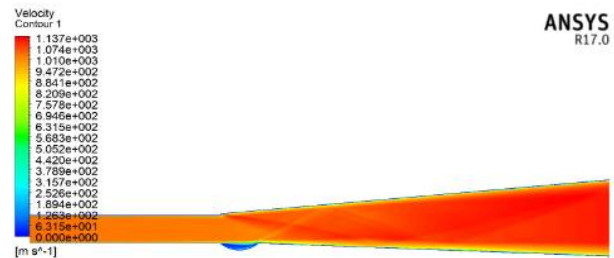


Fig 5.4b Velocity contours CircularCavities of L/D 5.5

The velocity contours for L/D ratio of 5.5 (open flow regime) is shown here, fig 5.4a shows the variation for rectangular cavity and fig 5.4b shows variation for circular cavity. In both the cases the velocity has been greatly reduced within the cavity. The contour shows a sub sonic region inside the cavity this region aids in flame holding and better flame stability. Thus open flow regime in both rectangular and circular cavity has given good results.

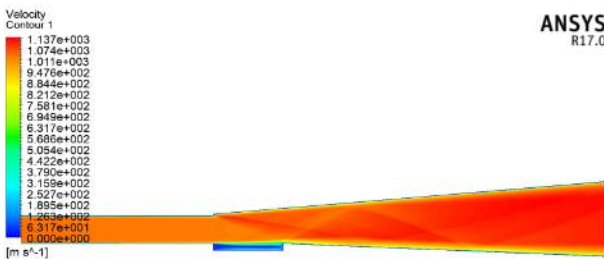


Fig 5.5a Velocity contours RectangularCavities of L/D 10

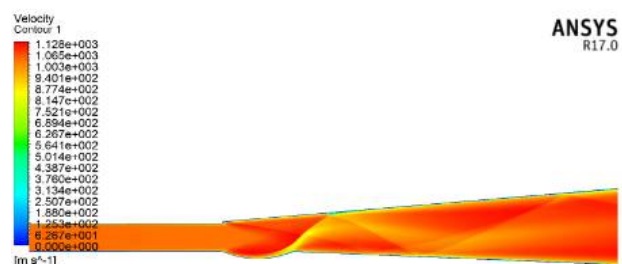


Fig 5.5b Velocity contours CircularCavities of L/D 10

The velocity contours for L/D ratio of 10 (transitional flow regime) is shown here, fig 5.5a shows the variation for rectangular cavity and fig 5.5b shows variation for circular cavity. It can be seen here that the rectangular cavity has still effectively reduced the velocity of flow within the cavity. While the circular cavity has not been effective in reducing the velocity of flow within the cavity. It can be observed here that the circular cavity a detached shear layer

and there is some noticeable reduction in velocity across it, but there in the rectangular cavity we don't have any shear layer within the cavity.

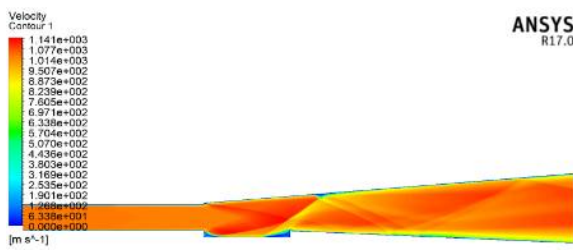


Fig 5.6a Velocity contours RectangularCavities of L/D 13

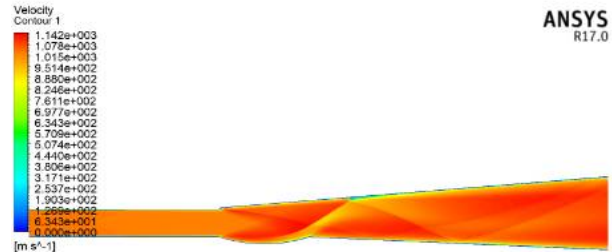


Fig 5.6b Velocity contours CircularCavities of L/D 13

The velocity contours for L/D ratio of 13 (closed flow regime) is shown here, fig 5.6a shows the variation for rectangular cavity and fig 5.6b shows variation for circular cavity. In rectangular cavity shear layer has entered the cavity and therefore the velocity is stagnating at the end walls of the cavity, because of which we can observe a subsonic region near the end walls of the cavity. In the circular cavity the velocity profile remains similar to transitional cavity flow along with the detached shear layer near the aft wall of the cavity.

Kerosene distribution

The results shown below given us an idea on how the fuel (kerosene) distribution occurs in the combustor for all cases of flow regimes.

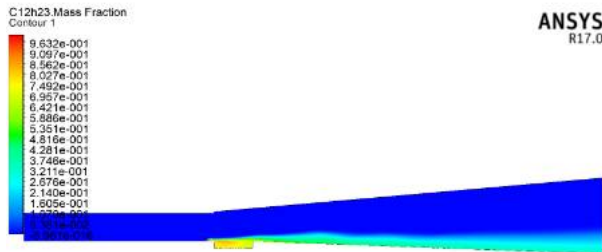


Fig 5.7a Kerosene distribution RectangularCavities of L/D 5.5

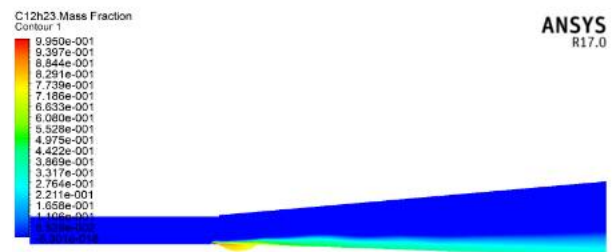


Fig 5.7b Kerosene distribution CircularCavities of L/D 5.5

The above contours shows fuel distribution in open cavity combustor for rectangular (fig 5.7a) and circular (fig 5.7b) flow regimes. Both the cavities in this flow regime have managed to effectively distribute the fuel within the combustor. Because there is no shear layer formation in the cavity the fuel is easily mixing with air in this case.

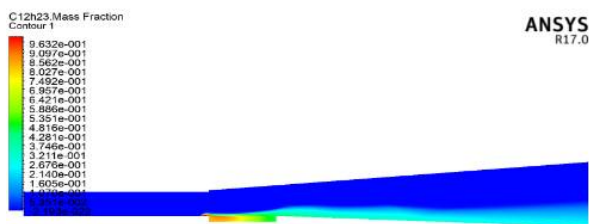


Fig 5.8a Kerosene distribution RectangularCavities of L/D 10



Fig 5.7b Kerosene distribution CircularCavities of L/D 10

The above contours shows fuel distribution in transitional cavity combustor for rectangular (fig 5.8a) and circular (fig 5.8b) flow regimes. In this case the fuel is distributed effectively in the rectangular cavity while the fuel has narrowed

down to a thin flow in circular cavity. We can observe a larger circulation zone being formed inside the rectangular cavity and it has held all components within it.

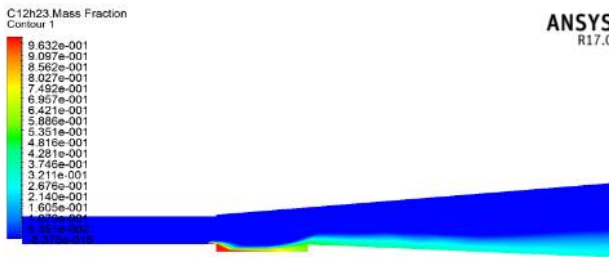


Fig 5.9a Kerosene distribution Rectangular Cavities of L/D 13

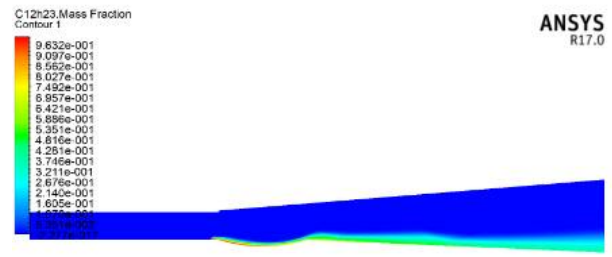


Fig 5.9b Kerosene distribution Circular Cavities of L/D 13

The above contours shows fuel distribution in closed cavity combustor for rectangular (fig 5.9a) and circular (fig 5.9b) flow regimes. We can observe the fuel stagnating near the end walls of the rectangular cavity, this is because the shear layer has entered inside the cavity and attached to the cavity floor. The fuel distribution in circular cavity is still narrow and thin. Based on the observations made from circular cavity, to prevent the fuel stagnating near end walls of rectangular cavity, we need to have an angled wall or an inclined surface near the end walls of the cavity

VI. VALIDATION STUDY

The computational results obtained might be off set from the actual case because of various parameters involved such as error in boundary conditions, inaccurate setup of computational model and also improper solver setting. Therefore, it is important to compare the obtained results with an already conducted experiment or a reputed numerical simulation. The simulation followed in here has been done with at most care and precision along with FLUENT convergence criteria.

Pressure variation along cavity wall

The cavity wall pressure measured in the computational result is shown in the fig 5.1a this is compared with the result obtained by Gruber et al [1]. Shown in the fig 5.1b. It can be observed that the pressure co-efficient along both the studies follows a similar graph. The pressure along the cavity floor remains constant up to cavity end wall. A strong flow ramming occurs at the end wall and a shock wave is formed hence there is drastic change in pressure gradient at the cavity end wall.

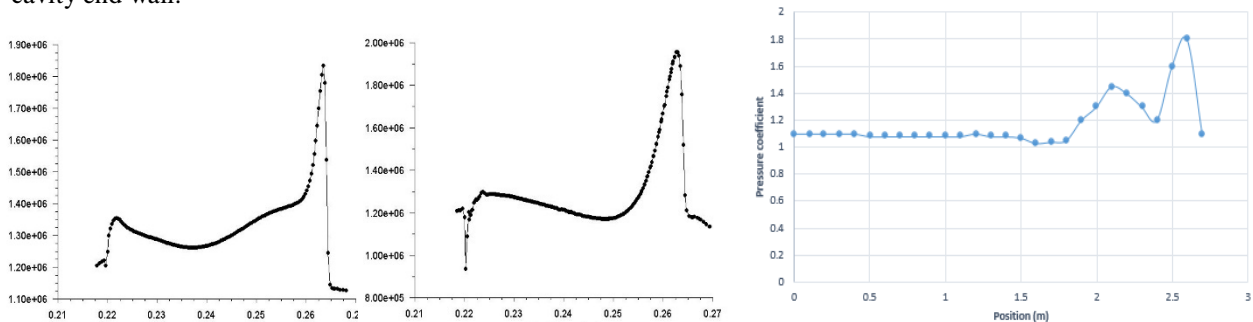


Fig 6.1a Computed Pressure along cavity wall rectangular-circular Fig 6.1b Pressure along cavity wall measured by Gruber et al.

Flow visualization

The experimental studies from Gruber et al [1] also employed flow visualization with techniques such as shadowgraph and schlieren flow visualization. The images shown below are from the study.

International Journal of Innovative Research in Science, Engineering and Technology

(A High Impact Factor, Monthly, Peer Reviewed Journal)

Visit: www.ijirset.com

Vol. 7, Issue 8, August 2018

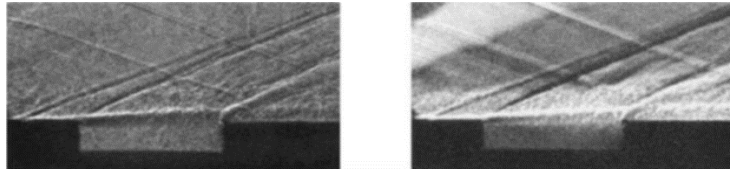


Fig 6.2a Shadowgraph and schlieren images

From the visualization it can be noted that there is a dark shock wave starting from the fore wall of the cavity. The next wave is the expansion wave that can be observed in the images, these images confirm the pressure co-efficient graphs obtained in the previous sections. The above flow visuals can be compared with the pressure contours obtained in the computation for both rectangular and circular cavities. The flow obtained in the computation agrees with the flow in the experimental flow visualization.

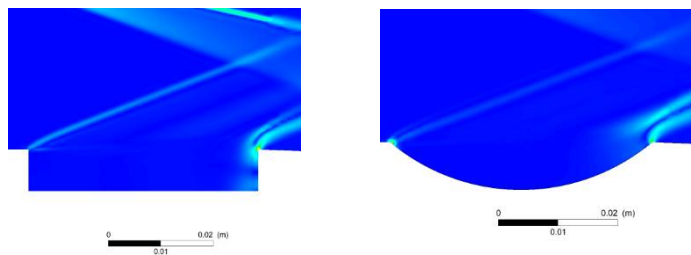


Fig 6.2b Computed images for rectangular and circular cavities

VII. CONCLUSION

1. The expansion wave and compression wave formation at the fore and aft wall in a rectangular cavity has been obtained like it was expected in the study carried out by Maureen B et al^[8]
2. The circular cavity behaved the same as rectangular cavity in open flow and it was different in closed and transitional cavity.
 - a) In transitional, the compression wave detaches from the cavity floor impinging the flow near aft wall
 - b) In closed cavity the flow was expected to enter cavity with a series of compression waves attached to the cavity floor, but it remained same as transitional flow with the compression wave sight changing its position towards the centre of the cavity, detached from the floor. This could be because of the geometric design of the cavity and since the cavity floor is curved we might need a larger L/D for the expected phenomena to occur
3. The cavity effect diminishes with increase in L/D and the results expected will overturn as we further increase it
 - a) To get quality results in rectangular cavity, the limit of L/D must stay in between open flows and transitional flows
 - b) To get quality results in circular cavity, the limit of L/D must stay in the open flow limit from the obtained computational result
 - c) If the combustor is designed using the parameters mentioned above, we obtain a subsonic region with-in the cavity which helps in flame holding.
4. It is evident that there is requirement for angled aft wall for larger L/D of rectangular cavity whereas the circular cavity in itself acts as an angled wall and hence we can see there is no formation of compression waves and shock impingement on the cavity floor.

International Journal of Innovative Research in Science, Engineering and Technology

(A High Impact Factor, Monthly, Peer Reviewed Journal)

Visit: www.ijirset.com

Vol. 7, Issue 8, August 2018

REFERENCES

- [1] Gruber, M. R., Baurle, R. A., Mathur, T., and Hsu, K. Y., "Fundamental Studies of Cavity Based Flame-Holder Concepts for Supersonic Combustors," *Journal of Propulsion and Power*, Vol. 17, No. 1, 2001, pp. 146–154.
- [2] Adela Ben-Yakar and Ronald K Hanson, "Cavity Flame holder for Ignition and Flame Stabilization in Scramjets: An Overview", *Journal of Propulsion and Power*, Vol.17, No.4, July-August-2001.
- [3] Arthur H. Lefebvre & Dilip R Ballal, "Gas Turbine Combustion Alternative Fuels and Emissions", 3rd Edition, CRC Press.
- [4] J. M. Beer and N. A. Chigier, *Combustion Aerodynamics*, Applied Science, London, 1972.
- [5] G. Yu, J. G. Li, X. Y. Chang, and L. H. Chen, "Fuel Injection and Flame Stabilization in a Liquid-Kerosene-Fueled Supersonic Combustor", *Journal Of Propulsion and Power*, Vol. 19, No. 5, September–October 2003.
- [6] Ben-Yakar, A., and Hanson, R. K., "Experimental Investigation of Flame-Holding Capability of a Transverse Hydrogen Jet in Supersonic Cross-Flow", *Proceedings of the Twenty-Seventh International Symposium on Combustion*, Combustion Inst., Pittsburgh, PA, 1998, pp. 2173–2180
- [7] Kyung Moo Kim ,SeungWookBaek , Cho Young Han "Numerical study on supersonic combustion with cavity-based fuel injection" *International Journal of Heat and Mass Transfer* 47 (2004) 271–286
- [8] Maureen B. Tracy and E. B. Plentovich, "Cavity Unsteady-Pressure Measurements at Subsonic and Transonic Speeds", *NASA Technical Paper* 3669, December 1997.
- [9] ZunCai, Xiaobin Zhu, Mingbo Sun, Zhenguo Wang "Experiments on flame stabilization in a scramjet combustor with a rear-wall-expansion cavity" *Science and Technology on Scramjet Laboratory*, National University of Defense Technology, Changsha, Hunan, 410073, China
- [10] Prateek Srivastava and K.M. Pandey "Computational analysis of supersonic combustion using cavity based fuel injection with species transport model at Mach number 4.17" *International Journal of Science, Environment ISSN 2278-3687 (O) and Technology*, Vol. 3, No 3, 2014, 923 – 930